NUREG/IA-0552

International Agreement Report

Analysis of CRDM Nozzle Break at the ATLAS Facility with 3D Components in MARS-KS and TRACE

Prepared by:
Hyunjoon Jeong*, Taewan Kim*, Jae Soon Kim**, Dong Gu Kang**

* Department of Safety Engineering, Incheon National University (INU)
119 Academy-ro, Yeonsu-gu,
Incheon, 22012, Republic of Korea

** Korea Institute of Nuclear Safety (KINS)
62 Gwahak-ro, Yuseong-gu,
Daejeon 34142, Republic of Korea

A. Hsieh, NRC Project Manager

Office of Nuclear Regulatory Research
U.S. Nuclear Regulatory Commission
Washington, DC 20555-0001

Manuscript Competed: December 2023
Date Published: June 2025

Prepared as part of
The Agreement on Research Participation and Technical Exchange
Under the Thermal-Hydraulic Code Applications and Maintenance Program (CAMP)

Published by
U.S. Nuclear Regulatory Commission

AVAILABILITY OF REFERENCE MATERIALS IN NRC PUBLICATIONS

NRC Reference Material

As of November 1999, you may electronically access NUREG-series publications and other NRC records at NRC's Library at www.nrc.gov/reading-rm.html. Publicly released records include, to name a few, NUREG-series publications; *Federal Register* notices; applicant, licensee, and vendor documents and correspondence; NRC correspondence and internal memoranda; bulletins and information notices; inspection and investigative reports; licensee event reports; and Commission papers and their attachments.

NRC publications in the NUREG series, NRC regulations, and Title 10, "Energy," in the *Code of Federal Regulations* may also be purchased from one of these two sources.

1. **The Superintendent of Documents**
   U.S. Government Publishing Office
   Washington, DC 20402-0001
   Internet: https://bookstore.gpo.gov/
   Telephone: (202) 512-1800
   Fax: (202) 512-2104

2. **The National Technical Information Service**
   5301 Shawnee Road
   Alexandria, VA 22312-0002
   Internet: https://www.ntis.gov/
   1-800-553-6847 or, locally, (703) 605-6000

A single copy of each NRC draft report for comment is available free, to the extent of supply, upon written request as follows:

Address: **U.S. Nuclear Regulatory Commission**
Office of Administration
Digital Communications and Administrative Services Branch
Washington, DC 20555-0001
E-mail: Reproduction.Resource@nrc.gov
Facsimile: (301) 415-2289

Some publications in the NUREG series that are posted at NRC's Web site address www.nrc.gov/reading-rm/doc-collections/nuregs are updated periodically and may differ from the last printed version. Although references to material found on a Web site bear the date the material was accessed, the material available on the date cited may subsequently be removed from the site.

Non-NRC Reference Material

Documents available from public and special technical libraries include all open literature items, such as books, journal articles, transactions, *Federal Register* notices, Federal and State legislation, and congressional reports. Such documents as theses, dissertations, foreign reports and translations, and non-NRC conference proceedings may be purchased from their sponsoring organization.

Copies of industry codes and standards used in a substantive manner in the NRC regulatory process are maintained at—

The NRC Technical Library
Two White Flint North
11545 Rockville Pike
Rockville, MD 20852-2738

These standards are available in the library for reference use by the public. Codes and standards are usually copyrighted and may be purchased from the originating organization or, if they are American National Standards, from—

American National Standards Institute
11 West 42nd Street
New York, NY 10036-8002
Internet: www.ansi.org
(212) 642-4900

Legally binding regulatory requirements are stated only in laws; NRC regulations; licenses, including technical specifications; or orders, not in NUREG-series publications. The views expressed in contractor prepared publications in this series are not necessarily those of the NRC.

The NUREG series comprises (1) technical and adminis-trative reports and books prepared by the staff (NUREG–XXXX) or agency contractors (NUREG/CR–XXXX), (2) proceedings of conferences (NUREG/CP–XXXX), (3) reports resulting from international agreements (NUREG/IA–XXXX),(4) brochures (NUREG/BR–XXXX), and (5) compilations of legal decisions and orders of the Commission and Atomic and Safety Licensing Boards and of Directors' decisions under Section 2.206 of NRC's regulations (NUREG–0750),and (6) Knowledge Management prepared by NRC staff or agency contractors.

NUREG/IA-0552

International Agreement Report

Analysis of CRDM Nozzle Break at the ATLAS Facility With 3D Components in MARS-KS and TRACE

Prepared by:
Hyunjoon Jeong*, Taewan Kim*, Jae Soon Kim**, Dong Gu Kang**

*Department of Safety Engineering, Incheon National University (INU)
119 Academy-ro, Yeonsu-gu,
Incheon, 22012, Republic of Korea

**Korea Institute of Nuclear Safety (KINS)
62 Gwahak-ro, Yuseong-gu,
Daejeon 34142, Republic of Korea

A. Hsieh, NRC Project Manager

Office of Nuclear Regulatory Research
U.S. Nuclear Regulatory Commission
Washington, DC 20555-0001
Manuscript Completed: December 2023
Date Published: June 2025

Prepared as part of
The Agreement on Research Participation and Technical Exchange
Under the Thermal-Hydraulic Code Applications and Maintenance Program (CAMP)

Published by
U.S. Nuclear Regulatory Commission

ABSTRACT

The Korea Atomic Energy Research Institute (KAERI) operates the Advanced Thermal-Hydraulic Test Loop for Accident Simulation (ATLAS), a facility designed to simulate transient and design basis accidents based on the Advanced Power Reactor 1400 (APR1400). Recently, a loss of coolant accident (LOCA) test at the top of the reactor pressure vessel (RPV) was conducted at ATLAS. This aimed to investigate the impact of losing safety injections (LSI) and evaluate accident management (AM) actions during such an event. An analysis of the ATLAS Control Rod Drive Mechanism (CRDM) nozzle break experiment was conducted using the MARS-KS and TRACE codes alongside their respective 3D components. The primary objective of this study is to investigate thermal-hydraulic phenomena during a small break LOCA at the RPV upper head with LSI. Additionally, it aims to assess the predictability of system analysis codes post AM actions during the test. The results are compared and discussed not only against experimental data but also with the calculation results of the VESSEL component, a 3D aspect of TRACE.

FOREWORD

The Korea Institute of Nuclear Safety (KINS) compiled this report under the Implementing Agreement on Thermal-Hydraulic Code Applications and Maintenance Program between the United States Nuclear Regulatory Commission (USNRC) and KINS (signed in 2023).

In 2023, KINS presented the results of this study at the 2023 Fall CAMP meeting and put forward the proposal as an in-kind contribution at the Technical Program Committee (TPC) meeting.

TABLE OF CONTENTS

ABSTRACT .... **iii**

FOREWORD .... **v**

TABLE OF CONTENTS .... **vii**

LIST OF FIGURES .... **ix**

LIST OF TABLES .... **xi**

EXECUTIVE SUMMARY .... **xiii**

ABBREVIATIONS AND ACRONYMS .... **xv**

1 INTRODUCTION **1**

2 DESCRIPTION OF THE ATLAS TEST **3**
- 2.1 ATLAS Experimental Facility 3
- 2.2 Test Condition 5

3 CODE MODELING AND PRELIMINARY ANALYSIS **7**
- 3.1 Description of Code Modeling 7
- 3.2 Results of RPV UH Node Sensitivity Analysis 12

4 RESULTS OF THE 3D MODEL **15**
- 4.1 Steady State Results 15
- 4.2 Transient Results 17

5 CONCLUSIONS **27**

6 REFERENCES **29**

LIST OF FIGURES

Figure 2-1 Schematic Diagram of the ATLAS Facility 5
Figure 2-2 Drawing of Installation Scheme of Break Line Simulation 6
Figure 3-1 ATLAS 1D Model Nodalization 9
Figure 3-2 Information of ATLAS 3D RPV Model 9
Figure 3-3 Renodalization of RPV UH 10
Figure 3-4 Break Module for ATLAS CRDM Nozzle Break 10
Figure 3-5 Comparison of Secondary System Heat Loss 11
Figure 3-6 Pressure of the Primary System According to Node Number (MARS-KS 1D) 13
Figure 3-7 Pressure of the Primary System According to Node Number (TRACE 1D) 13
Figure 3-8 PCT According to Node Number (MARS-KS 1D) 14
Figure 3-9 Comparison of the Secondary System Heat Loss (TRACE 1D) 14
Figure 4-1 Comparison of the Volumes for RPV with MultiD and Vessel Components 17
Figure 4-2 Power of the Core Heater (3D) 21
Figure 4-3 Integrated Break Flow (3D) 21
Figure 4-4 Pressure of the Primary System (3D) 22
Figure 4-5 Active Core Collapsed Water Level (3D) 22
Figure 4-6 Peak Cladding Temperature (3D) 23
Figure 4-7 RCP Side IL Collapsed Water Level of Experiment 23
Figure 4-8 RCP Side IL Collapsed Water Level of MARS-KS (3D) 24
Figure 4-9 RCP Side IL Collapsed Water Level of TRACE (3D) 25
Figure 4-10 Active Core Collapsed Water Level and PCT (1,500~2,500 Sec) 25

LIST OF TABLES

Table 2-1 Major Scaling Parameters of ATLAS 4
Table 4-1 Steady State Results 16
Table 4-2 3D Chronology of the Transient Main Events..20
Table 4-3 Results of the FFTBM Analysis...26

EXECUTIVE SUMMARY

This report presents an analysis of the CRDM nozzle break SBLOCA with SIP unavailability in the ATLAS facility. The experiment was analyzed by the thermal-hydraulic system codes, MARS-KS 2.0 and TRACE 5.0 Patch 7. This assessment aimed to evaluate the predictability of the 3D component. The calculation results are compared and discussed not only against the experiment but also against the calculation results of both codes. Additionally, preliminary sensitivity analysis results have been presented for the stratification effect of the upper head.

The analysis has been conducted through 3 stages:

1. Initially, the analysis involved developing 1D and 3D models based on reference input, with both models implemented identically, except for the RPV. To minimize modeling differences between the codes, nodalization was created using the same approach. Moreover, a break system was designed, encompassing a break nozzle, valve, sink volume, and pipes, to simulate CRDM nozzle rupture. Accurate break flow prediction utilized critical flow models, and a new correlation for heat loss on the secondary side was developed.

2. Subsequently, preliminary sensitivity analysis was performed using the 1D component. When implementing the RPV UH with a single control volume, inadequate simulation of the stratification phenomenon in the upper RPV led to inaccurate break flow predictions. This inaccuracy resulted in a rapid decrease in system coolant inventory and fast depressurization, failing to accurately predict overall system behavior. To address these limitations, a sensitivity analysis was conducted for the RPV UH control volume by dividing it into subvolumes. Based on these findings, the same methodology was applied to the 3D model, simulating the upper part of the reactor pressure vessel using a total of 14 axial nodes in the calculations.

3. In the third stage, steady-state calculations and transient state simulations were performed using the 3D models of each code (MARS-KS: MultiD component, TRACE: Vessel component). The 3D ATLAS models in each code followed the same approach as the 1D ATLAS modeling, differing only in the RPV model. Here, the analysis involved scrutinizing the MARS-KS 3D and TRACE 3D calculation results through code-to-code comparison.

The primary focus of this report is investigating thermal-hydraulic phenomena during an SBLOCA at the RPV upper head with LSI, along with assessing the predictability of the system analysis codes utilizing the 1D and 3D components, respectively.

The key findings from comparing the MARS-KS 3D and TRACE 3D results with the ATLAS CRDM nozzle break experiment are:

The results from the steady-state 3D calculations indicate accurate prediction of most major parameters, well within acceptable error margins. However, the SG pressure showed the highest error at 3.18% in both calculations. Analyzing secondary system parameters revealed that the saturation pressure corresponding to the steam temperature exceeded the measured SG pressure. This suggested that if the secondary condition were controlled by SG pressure, the SG temperature would be lower than the experimental result, consequently leading to a lower core inlet temperature, as confirmed by preliminary analysis.

Node sensitivity results indicated that treating the upper part of the RPV as a single volume in the reference model resulted in a more rapid primary system pressure decrease due to inadequate simulation of stratification. Detailed node modeling of the upper volume produced a more appropriate pressure behavior prediction. The detailed node model accurately predicted coolant inventory and primary system pressure, directly affecting the PCT and suggesting an appropriate AM action response. These findings emphasize the necessity of renodalizing the UH volume of the RPV to accurately capture physical phenomena.

Therefore, the 3D RPV modeling was executed using the same approach as the 1D nodalization of the RPV upper head. The results indicated that both codes appropriately predicted the overall physical behaviors of the system during the accident.

Overall, the transient behavior in 3D for both codes exhibited similar system behavior, except regarding the formation of the loop seal and its influence on the system. In the 3D calculation of both codes, the integrated break flow and primary system pressure behavior until ADV opening accurately matched the experimental results. The timing of ADV opening correlated directly with core heat-up and the behavior of the active core collapsed water level, which varied depending on the loop seal behavior. Although the 3D calculations of both codes did not precisely replicate the loop seal behavior of the experiment, the physical phenomena resulting from the loop seal were appropriately captured in both simulations.

ABBREVIATIONS AND ACRONYMS

ADV	Atmospheric Dump Valve
AFW	Auxiliary Feed Water
AM	Accident Management
ATLAS	Advanced Thermal-hydraulic Test Loop for Accident Simulation
CL	Cold Leg
CRDM	Control Rod Drive Mechanism
DBA	Design Basis Accident
DC	Downcomer
DP	Differential Pressure
DSP	Domestic Standard Problem
DVI	Direct Vessel Injection
ECCS	Emergency Core Cooling System
FLB	Feed Line Break
FFTBM	Fast Fourier Transform Based Method
HL	Hot Leg
IL	Intermediate Leg
KAERI	Korea Atomic Energy Research Institute
KINS	Korea Institute of Nuclear Safety
LBLOCA	Large Break Loss of Coolant Accident
LSI	Loss of Safety Injection
LOCA	Loss of Coolant Accident
LSC	Loop Seal Clearing
LPP	Low Pressurizer Pressure
MFIV	Main Feedwater Isolation Valve
MSIV	Main Steam Isolation Valve
MSLB	Main Steam Line Break
MSSV	Main Steam Safety Valve
PCT	Peak Cladding Temperature
PWSCC	Primary Water Stress Corrosion Cracking
PZR	Pressurizer
RCP	Reactor Coolant Pump
RCS	Reactor Cooling System
RPV	Reactor Pressure Vessel

SBLOCA	Small Break Loss of Coolant Accident
SG	Steam Generator
SGTR	Steam Generator Tube Rupture
SIS	Safety Injection System
SIP	Safety Injection Pump
SIT	Safety Injection Tank
UH	Upper Head

1 INTRODUCTION

After the Fukushima accident, ensuring safety under multiple-failure conditions became paramount. Specifically, the failure of safety injection is viewed as a potential scenario that could lead to core damage if not addressed properly.

PWSCC was discovered in the nozzle of the CRDM penetration at Hanbit Unit 3 [1]. Additionally, cracks were identified at the welds on the upper head penetration nozzle of the RPV at Hanbit Unit 5 during preventive maintenance [2]. The circumferential cracking of CRDM penetration nozzles could potentially cause an SBLOCA at the RPV upper head. The thermal-hydraulic behavior during an SBLOCA at the RPV upper head differs somewhat from other SBLOCAs due to the primary flow being in the vapor phase.

Studies indicate that even in an SBLOCA at the RPV upper head, the coolant inventory in the primary system is relatively preserved through safety injection, effectively delaying core heat-up [3]. However, an SBLOCA at the RPV upper head without safety injections could lead to core damage unless appropriate AM actions are taken.

KAERI operates an integral effect test facility, ATLAS, referencing the APR1400 for transient experiments and DBA simulations. An experimental study on an SBLOCA at the RPV upper head with safety injection failure was conducted at ATLAS to address safety concerns and evaluate AM effectiveness. The experimental data were used to validate various system codes within the DSP-06 framework, organized by KAERI in collaboration with KINS [4].

In this study, the experiment was analyzed using thermal-hydraulic system codes, MARS-KS [5] and TRACE [6]. The analysis focused on thermal-hydraulic phenomena during the SBLOCA at the RPV upper head with LSI, alongside the predictability of system codes post-AM actions. Additionally, it evaluated the predictability of 3D components, and the calculation results were compared and discussed against the experiment.

2 DESCRIPTION OF THE ATLAS TEST

2.1 ATLAS Experimental Facility

The ATLAS is a thermal-hydraulic integral test facility referencing the APR1400. The reference plant for ATLAS is the APR1400, an advanced power reactor developed by the Korean nuclear industry, featuring a rated thermal power of 4000 MW and a loop arrangement of two HLs and four CLs for the reactor coolant system. ATLAS allows the investigation of system responses for the overall plant or subcomponents in a specific system during anticipated transients and postulated accidents [7]. Equipped with approximately 1,600 measuring instruments, ATLAS measures system parameters during postulated accidents [8].

ATLAS has been designed based on the three-level scaling methodology suggested by Ishii and Kataoka [9], aiming to simulate various test scenarios as realistically as possible. Sharing the same two-loop features as APR1400, ATLAS is a half-height and volume scale of 1/288 test facility, following the scaling law where reducing the height results in a time reduction in the model. For a facility with one-half height, the time for the scaled model is 1.4 times faster than the prototypical time. The friction factors in the scaled model are maintained to be the same as those of the prototype. The hydraulic diameter of the scaled model is also maintained to be the same as that of the prototype to preserve prototypical conditions for the heat transfer coefficient. The major scaling parameters of ATLAS are summarized in Table 2-1 [10].

The thermal power of ATLAS is simulated by electrical heater rods, with a maximum power of 1.96 MW, equivalent to 10% of the scaled power. Figure 2-1 illustrates a schematic diagram of the ATLAS facility, comprising the RCS, secondary system, safety injection system, AFW system, break simulation, and containment. The primary system of ATLAS includes an RPV, a PZR, two HLs, four CLs, four RCPs, and two SGs. The SIS of ATLAS consists of four SIPs and four SITs capable of simulating safety injection and long-term cooling, a charging pump for auxiliary spray, and a shutdown cooling pump and a shutdown heat exchanger for low-pressure safety injection, shutdown cooling operation, and recirculation operation.

The break simulation system consists of several break simulating lines, including LBLOCA, DVI line break LOCA, SBLOCA, SGTR, MSLB, and FLB, etc. Detailed design information and a description of the ATLAS facility can be found in the facility description report [11].

Table 2-1 Major Scaling Parameters of ATLAS

Parameter	Scaling law	ATLAS Design
Length	l_{OR}	1/2
Diameter	d_{OR}	1/12
Area	d_{OR}^2	1/144
Volume	$l_{OR}d_{OR}^2$	1/288
Core DT	ΔT_{OR}	1
Velocity	$l_{OR}^{1/2}$	$1/\sqrt{2}$
Time	$l_{OR}^{1/2}$	$1/\sqrt{2}$
Power/Volume	$l_{OR}^{-1/2}$	$\sqrt{2}$
Heat Flux	$l_{OR}^{-1/2}$	$\sqrt{2}$
Core Power	$l_{OR}^{1/2}d_{OR}^2$	1/203.6
Flow Rate	$l_{OR}^{1/2}d_{OR}^2$	1/203.6
Pressure Drop	l_{OR}	1/2

where *l* is the length, *d* is the diameter, and *T* is the temperature

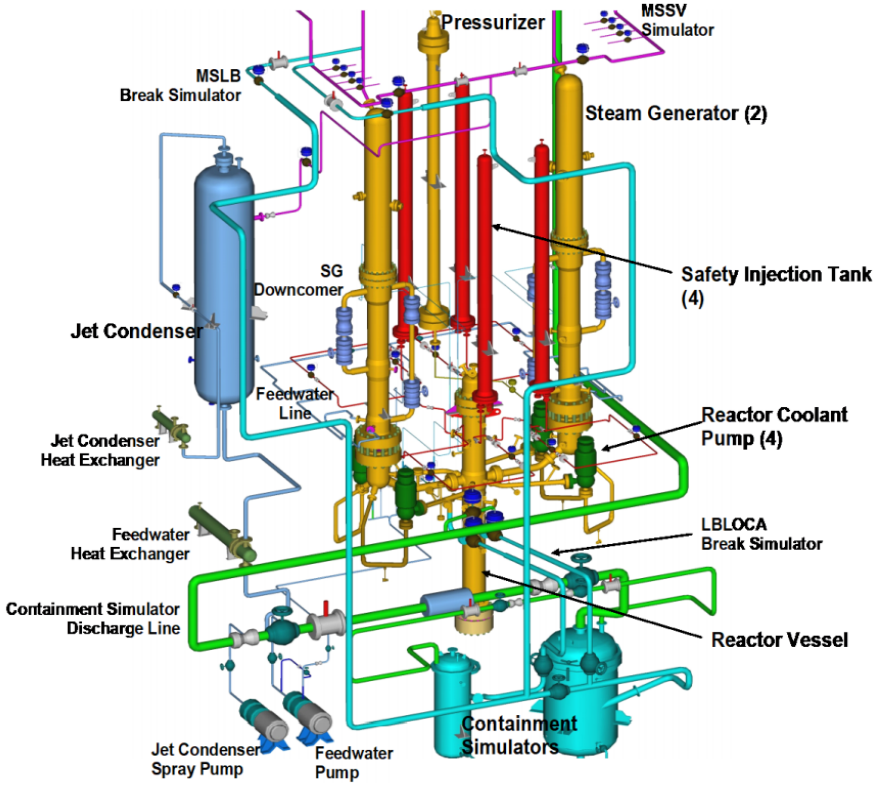

Figure 2-1 Schematic Diagram of the ATLAS Facility

2.2 Test Condition

During the test, four SITs were activated as part of the safety system, while the SIPs remained inactive to simulate total SIP failure. Secondary safety systems, such as MSSVs and AFW, were assumed to be available. Additionally, the ADV was activated to implement the AM action and set to open at 50% valve stem position when the AM action was utilized. Since the experiment was conducted under conditions surpassing the DBA, the core protection system was eligible for activation, safeguarding the heater rods from damage. To establish experimental conditions independent of the core protection system, a series of preliminary experiments were conducted. These aimed to determine the ADV opening conditions, concluding that the ADV should open when the surface temperature of the heater rods in the core exceeded 623.15K.

AFW injection commenced and ceased when the SG collapsed water level reached 25% and 40% of the nominal level, respectively. AFW temperature and flow rate were set at 323.15 K and 0.198 kg/s, respectively. The SITs were delivered through the DVI nozzles at the DC of the RPV, maintaining a temperature of 323.15 K, level at 3.7 m, and pressure at 4.3 MPa. Initial heater power was controlled at 1.664 MW, and decay heat was simulated using the ANS-73 decay curve with a multiplier of 1.2. To simulate a break at the UH, a break line simulation was installed, as depicted in Figure 2-2. The inner diameter of the break nozzle was determined to be 7.12mm, corresponding to the break area for two CRDM nozzles of the APR1400 [4].

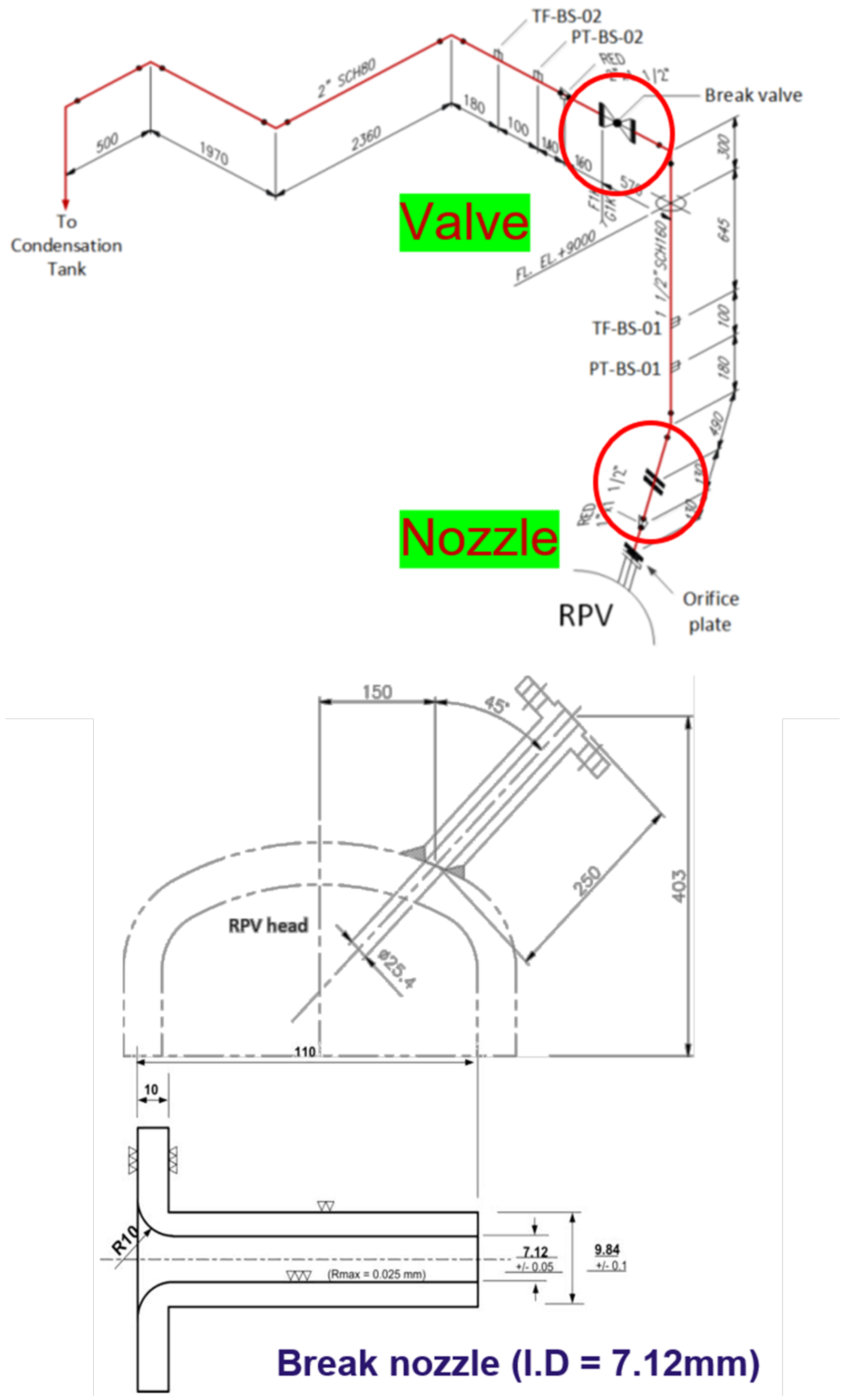

Figure 2-2 Drawing of Installation Scheme of Break Line Simulation

3 CODE MODELING AND PRELIMINARY ANALYSIS

3.1 Description of Code Modeling

For this analysis, one-dimensional (1D) and three-dimensional (3D) models (referred to as 1D and 3D models in this report) were developed based on the reference input [11]. To verify whether the geometric and thermal structure information of the reference input was consistent with the actual design information, the design values presented in the technical report were compared with the reference input. Upon review, discrepancies were identified in the volume of the RPV lower plenum, heat structure information of the primary system piping, and heat structure information of the SG economizer. These input error values were corrected/reflected based on the design values presented in the technical report.

Information regarding the 1D and 3D models is presented in Figures 3-1 and 3-2, respectively, where the areas highlighted in red indicate the areas where the mentioned errors were corrected. The 1D and 3D models are identical except for the reactor pressure vessel, and the axial height of the reactor pressure vessel in the axial direction is implemented identically in both the 1D and 3D models. The upper head of the reactor pressure vessel in each model is reconstructed with a total of 14 axial nodes, based on the conclusions drawn from preliminary calculations of the 1D model. Detailed information is provided below.

In Figure 3-1, the 1D reference model implemented the upper part of the RPV using a single control volume. However, given the break at the top of the RPV, it was evident that the upper RPV section would be stratified during the accident. These effects posed limitations in accurately predicting overall break flow and pressure behavior. To address this, a sensitivity analysis divided the control volume of the RPV upper head in detail during a 1D preliminary analysis, which was then applied to 3D calculations. The model, depicted in Figure 3-3, divided the upper head into 14 subvolumes and was selected as the final model. Further discussion is available in the subsequent section.

For simulating the CRDM nozzle rupture at the UH, a break system was implemented atop the RPV. The objective was to design this system to closely mirror the test configuration, ensuring an accurate prediction of the transient characteristics of the break flow. The components within the break system included a break nozzle, break valve, sink volume, and break pipes, illustrated in Figure 3-4.

Among these components, modeling the break nozzle was particularly crucial for this simulation. Choking in the break line was expected to occur at its narrowest section. The break nozzle had the smallest inner diameter within the break line, measuring 7.12 mm, while the inner diameter of the break pipeline measured 33.99 mm. Therefore, the Henry-Fauske critical flow model [13], default in MARS-KS, was applied at the break nozzle. Similarly, in TRACE, the Ransom-Trapp critical flow model [14] was also applied at the break nozzle. To ensure an appropriate prediction of integrated break flow, the discharge coefficient for MARS-KS's 1D model was set to 0.8, while for TRACE's 1D model, subcooled and two-phase discharge coefficients were set to 0.5 and 0.8, respectively. For the 3D models, the discharge coefficient in MARS-KS was set to 1.0, and in TRACE, subcooled and two-phase discharge coefficients were both set to 0.9.

The total heat loss in the primary system was calculated by combining the heat losses from the RPV and the primary piping. This heat loss was quantified as a function of wall temperature derived from a separate heat loss test [12]. The correlation used is as follows:

$$Q_{loss,P} = 0.091 \cdot (T_w - T_{atm})^{5/4} \tag{3-1}$$

where, T_w and T_{atm} denote the temperatures of the wall and atmosphere, respectively. On the secondary side, we accounted for heat losses from the outer shells of SGs and main steam lines. These losses were determined based on the temperature difference between the walls and the surrounding atmosphere, using a similar approach to that employed on the primary side [12]. However, the temperature difference in the steady state of the postulated scenario exceeded the range covered by the correlation for secondary heat loss. Extrapolating this correlation could not accurately predict the heat loss estimated from the experimental results. Consequently, a new correlation was developed using a 4th order polynomial that fits the data from the separate heat loss test and targets the value for this experiment, outlined as follows:

$$\begin{aligned} Q_{loss,s} = 281.410 - 5.52175 \cdot \Delta T + 0.04063 \cdot (\Delta T)^2 \\ -1.2927 \times 10^{-4} \cdot (\Delta T)^3 + 1.55502 \times 10^{-7} \cdot (\Delta T)^4 \end{aligned} \tag{3-2}$$

where, $\Delta T = T_w - T_{atm}$. The newly developed correlation effectively captures the overall trend of heat loss, showcasing a remarkably high adjusted R-squared value of 0.99993, as depicted in Figure 3-5. This new correlation was adopted for this study to accurately estimate heat losses from the secondary system.

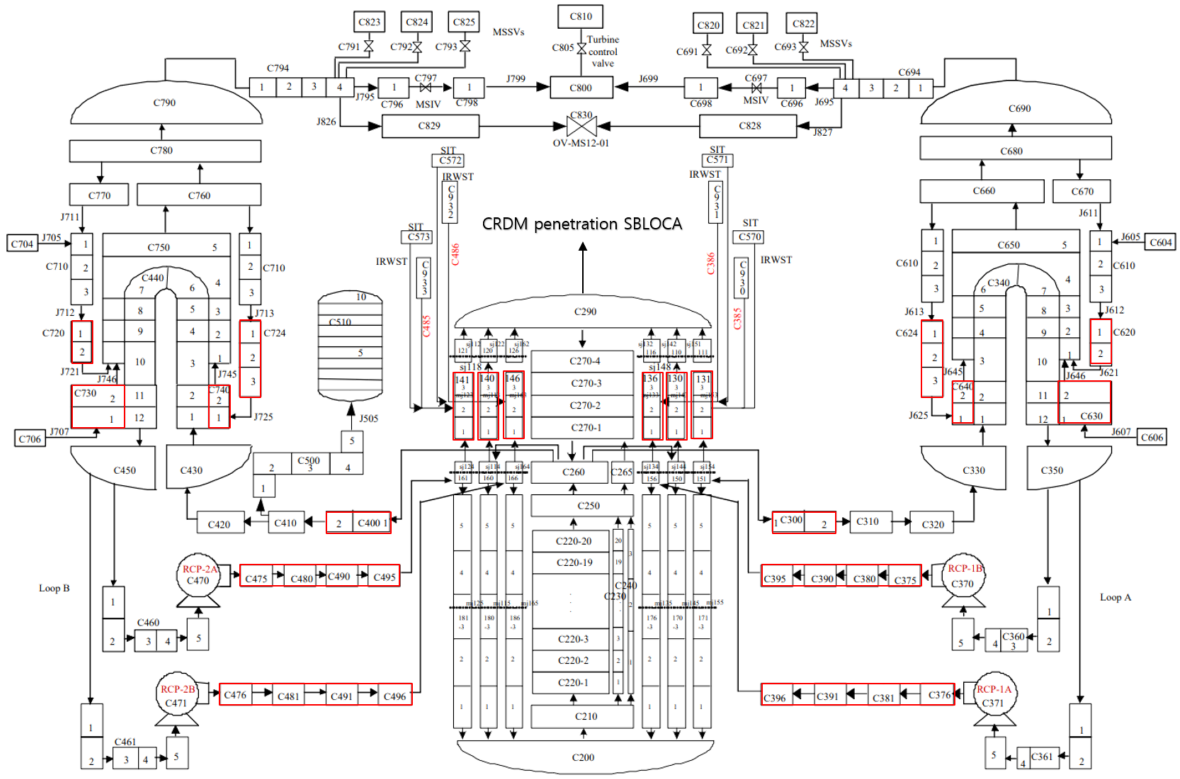

Figure 3-1 ATLAS 1D Model Nodalization

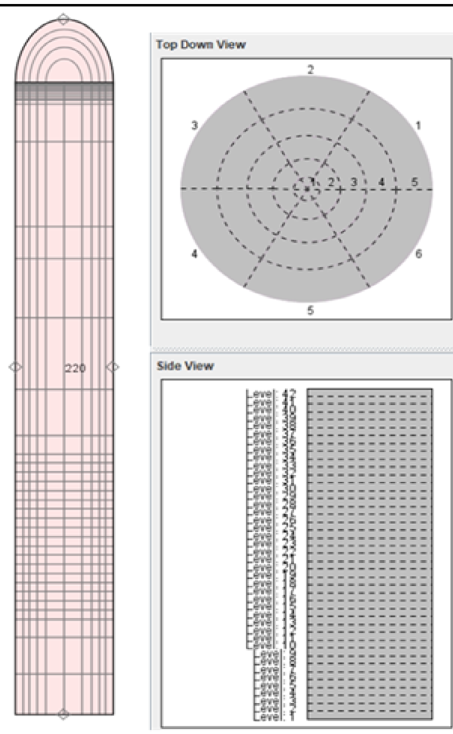

Radial Ring	Reference
1	Core
2	
3	
4	Core bypass
5	Downcomer

Axial Level	Reference
29~42	Upper Head
25~28	Upper downcomer
24	Upper plenum
23	Core outlet region
3~22	Active core
2	Core inlet
1	Lower plenum

Figure 3-2 Information of ATLAS 3D RPV Model

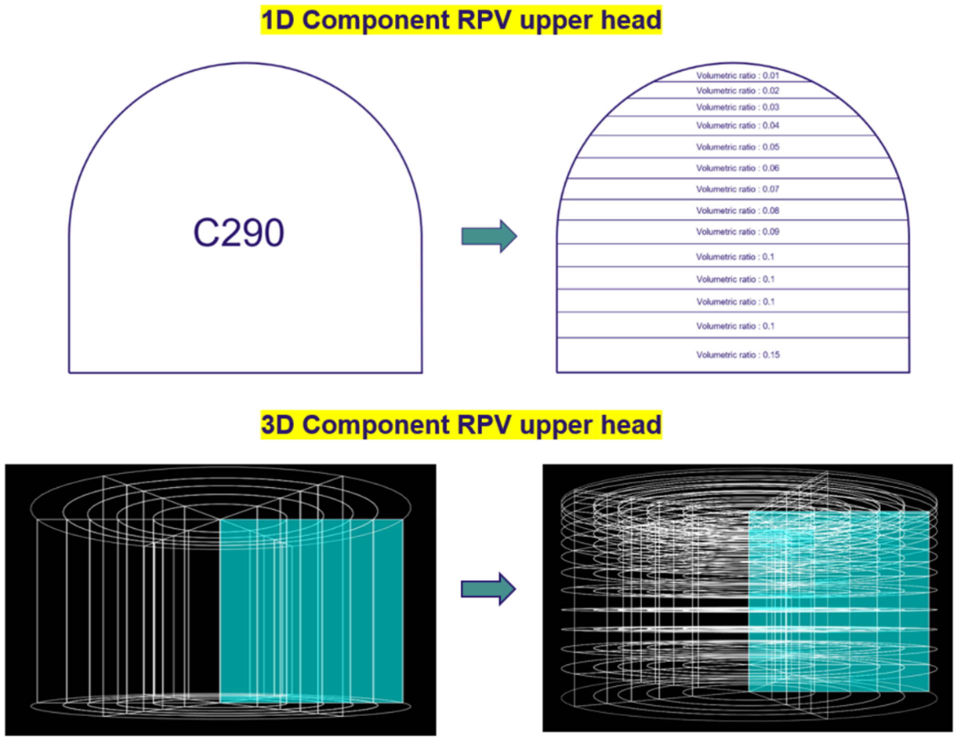

Figure 3-3 Renodalization of RPV UH

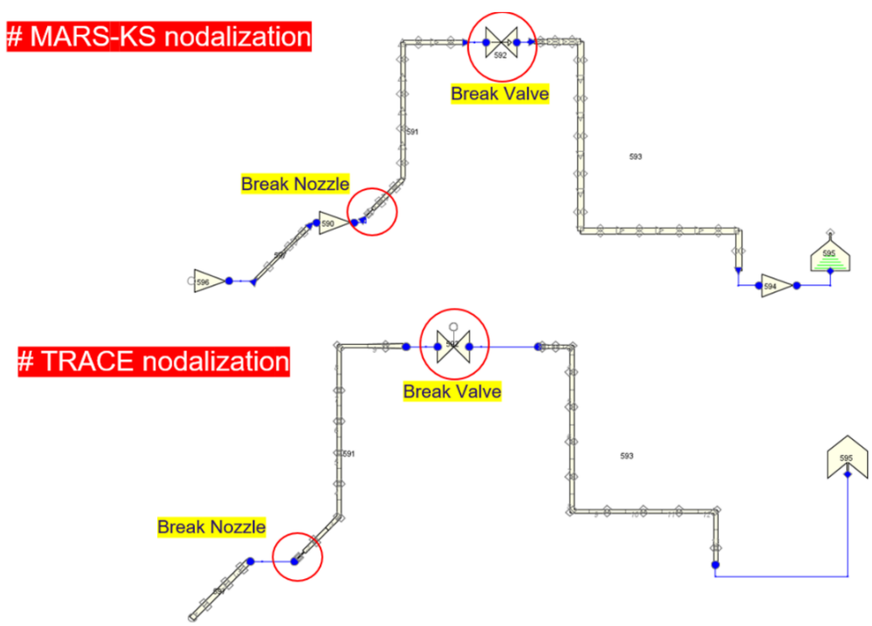

Figure 3-4 Break Module for ATLAS CRDM Nozzle Break

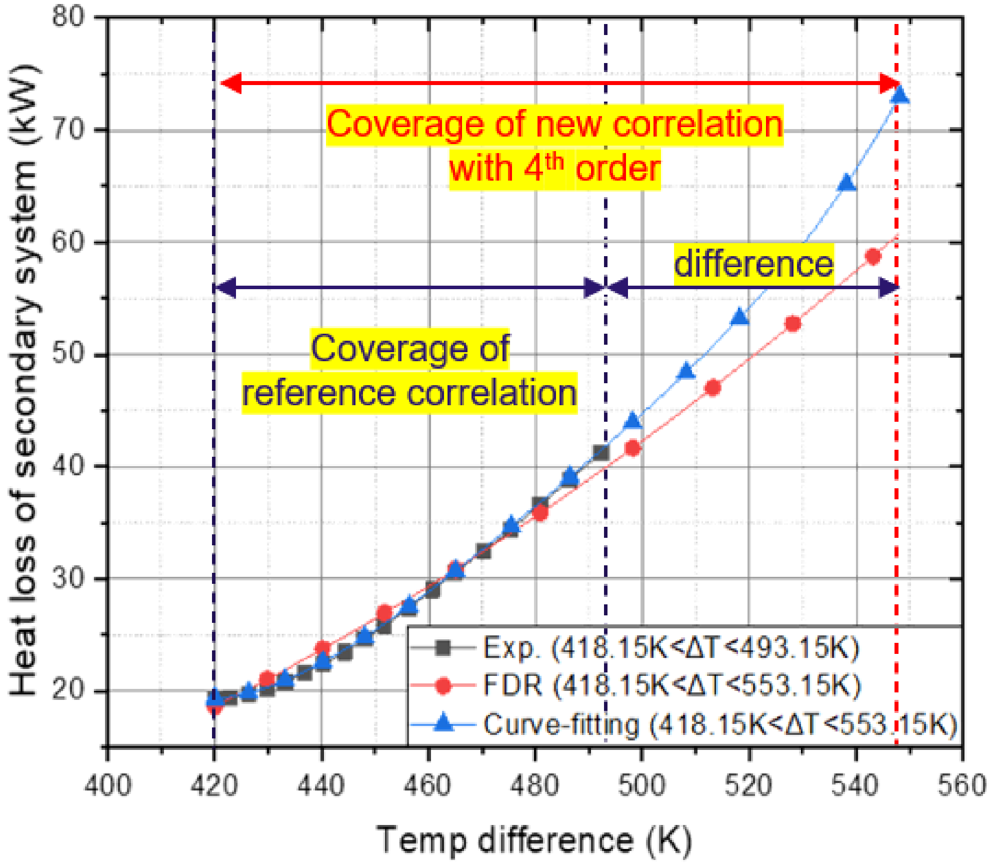

Figure 3-5 Comparison of Secondary System Heat Loss

3.2 Results of RPV UH Node Sensitivity Analysis

As previously mentioned, an accurate prediction of the break flow from the RPV UH requires proper modeling. The ATLAS experiment simulates the condition of coolant being discharged through the RPV UH, where it is evident that the fluid in the upper part of the RPV could be stratified. However, when implementing the UH using a single control volume, such as the 1D reference model, it fails to adequately simulate this stratification phenomenon, resulting in an inaccurate prediction of the break flow.

In other words, even when single-phase gas is discharged, the simulation shows abnormal fluid discharge, leading to an over-prediction of the break flow rate. This inaccuracy in predicting the break flow results in a rapid decrease in the system coolant inventory and fast depressurization, which decreases the accuracy of prediction of the system behavior. Therefore, to address the limitations of the reference model and to predict the break flow rate considering stratification more accurately, a sensitivity analysis was conducted for the upper head control volume of the RPV.

The sensitivity analysis was conducted by dividing the volume of the RPV UH into 5, 10, and 14 sub-volumes, including the single-volume reference model, and the results are presented in Figures 3-6 to 3-9. As observed in Figures 3-6 and 3-7, when the upper part of the RPV was implemented as a single volume in the reference model, the primary system pressure decreased more rapidly. This is attributed to the inability of the reference model to adequately simulate the stratification phenomenon in the upper part of the RPV, leading to the release of more coolant through the break line.

In case the upper volume of the pressure vessel was modeled with more detailed nodes, a more appropriate pressure behavior could be predicted. Since the coolant inventory and primary system pressure behavior are directly related to the PCT, the detailed node model predicted the correct behavior of these parameters, resulting in an appropriate PCT behavior, as shown in Figures 3-8 and 3-9.

These results demonstrate a need to renodalize the UH volume of the RPV to consider the physical phenomena occurring in the experiment accurately. Based on these findings, the same methodology was applied to the 3D model, simulating the upper part of the reactor pressure vessel with a total of 14 axial nodes and utilizing it in the calculations.

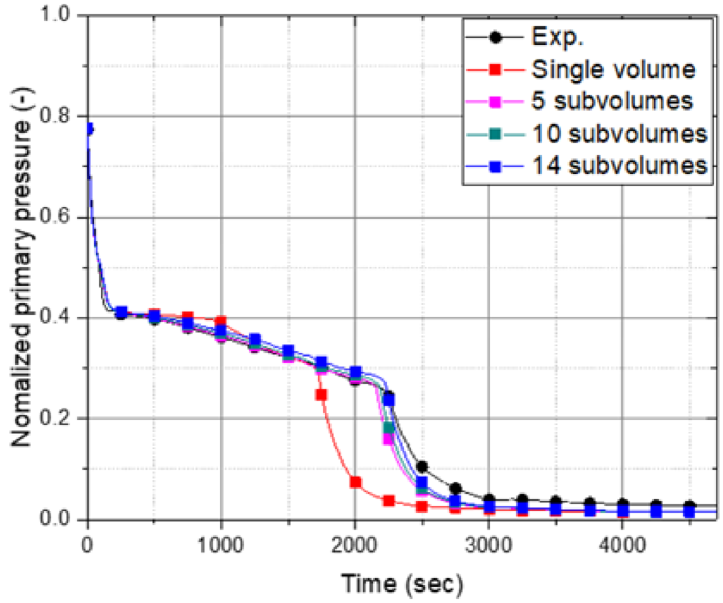

Figure 3-6 Pressure of the Primary System According to Node Number (MARS-KS 1D)

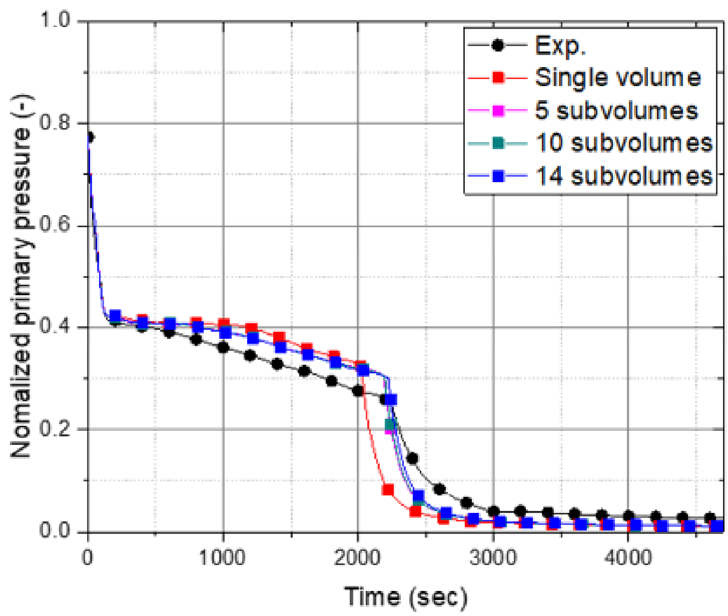

Figure 3-7 Pressure of the Primary System According to Node Number (TRACE 1D)

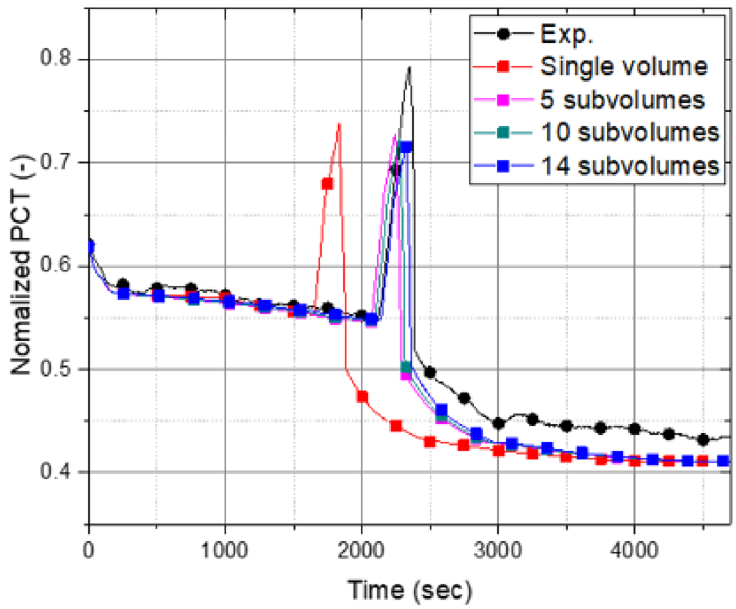

Figure 3-8 PCT According to Node Number (MARS-KS 1D)

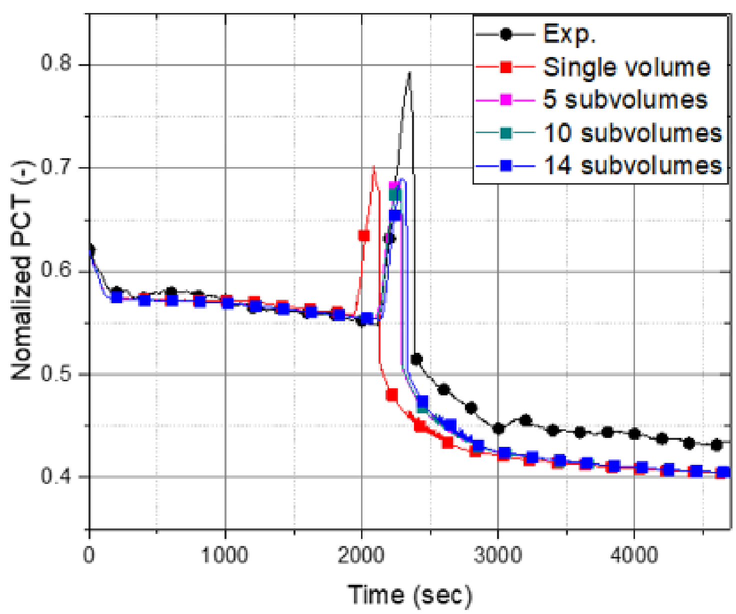

Figure 3-9 Comparison of the Secondary System Heat Loss (TRACE 1D)

4 RESULTS OF THE 3D MODEL

4.1 Steady State Results

A steady-state calculation of the 3D model was conducted over 5,000 seconds to establish initial conditions for the anticipated accident. The summary of the steady-state calculations using MARS-KS and TRACE is presented in Table 4-1.

As mentioned earlier, the 3D model of the RPV employed the MultiD component (MARS-KS) and the Vessel component (TRACE), while the control volumes, apart from the RPV, utilized the same 1D model. Moreover, a comparison between the reactor pressure vessel volumes implemented using MARS-KS MultiD and TRACE Vessel components confirmed their alignment with the values specified in the experimental specifications, as depicted in Figure 4-1.

Most major parameters were accurately predicted and fell within acceptable error margins, except for SG pressure, which exhibited the highest error at 3.18% in both calculations. Analysis of secondary system parameters revealed that the saturation pressure corresponding to the steam temperature surpassed the measured SG pressure. Consequently, it became evident that if the secondary condition was controlled by SG pressure, the SG temperature would be lower than the experimental result. This would inherently lead to a lower core inlet temperature, as affirmed by a preliminary analysis [15].

Table 4-1 Steady State Results

Parameter	Experiment	Calculated		Error [%]	
		MARS-KS	TRACE	MARS-KS	TRACE
Primary System					
Core Power (MW)	1.66	1.66	1.66	0.00	0.00
Heat Loss (kW)	98.4	98.1	98.1	-0.41	-0.41
PZR Pressure (MPa)	15.5	15.5	15.5	0.00	0.00
PZR Level (m)	3.62	3.62	3.62	0.00	0.00
Core Inlet Temp. (K)	565.35	564.45	564.50	-0.16	-0.12
Core Outlet Temp. (K)	600.95	600.95	600.25	0.00	-0.12
Secondary System					
Feed Water Flow Rate (kg/s)	SG 1:0.41 SG 2:0.42	SG 1:0.41 SG 2:0.42	SG 1:0.42 SG 2:0.42	SG 1:0.00 SG 2:0.00	SG 1:2.14 SG 2:0.00
Feed Water Temp. (K)	506.45	506.45	506.45	0.00	0.00
Steam Pressure (MPa)	7.83	8.0795	8.0795	3.18	3.18
Steam Temp. (K)	SG1:569.35 SG2:568.35	SG 1:568.85 SG 2:568.85	SG 1:568.85 SG 2:568.85	SG 1:-0.09 SG 2:0.09	SG 1:-0.09 SG 2:0.09
Secondary Side Level (m)	4.99	4.99	5.05	0.00	1.20
Heat Loss (kW)	70.0	69.9	70.1	-0.14	0.14
Primary Piping					
Cold Leg Flow (kg/s)	2.0	1.94	1.99	-3.00	-0.05

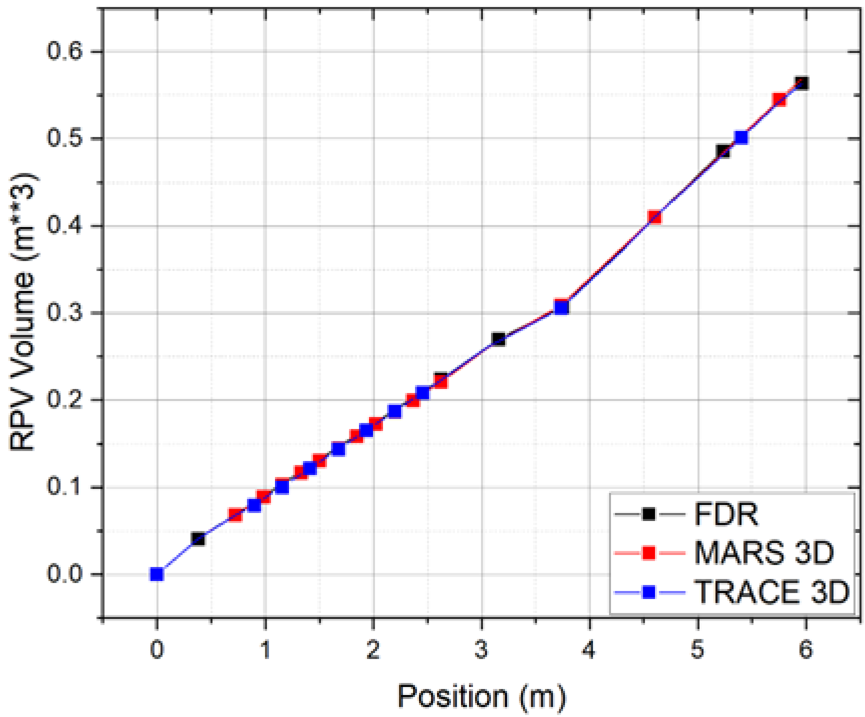

Figure 4-1 Comparison of the Volumes for RPV with MultiD and Vessel Components

4.2 Transient Results

The analysis of CRDM nozzle break was conducted under steady state conditions using the 3D component. Table 4-2 presents a chronology of the main events during the CRDM SBLOCA test, comparing the results from the experiment with those from both codes. The CRDM SBLOCA was initiated by opening the break valve at 0.0 seconds. In the early stages of the accident, the primary system rapidly depressurized, leading to a reactor trip triggered by the LPP signal. Concurrently, the secondary system was isolated through the activation of the MSIS and MFIS, following predefined delays from the reactor trip signal. Figure 4-2 illustrates the core power, representing the decay heat curve simulated with 3D components in MARS-KS and TRACE. The core power in ATLAS corresponded to 8% of the scaled nominal power.

Figure 4-3 depicts the integrated break flow through the break valve in the 3D calculation. The figure suggests that both codes provided a good prediction of the break flow until the opening time of the ADV. The initial blowdown region witnessed the discharge of single-phase liquid; subsequently, a less steep depressurization region formed due to two-phase flow in the brake module. Afterwards, as the void fraction of the break module increased, the break flow transitioned from two-phase flow to single-phase vapor. The 3D calculations of both codes appropriately predicted the integrated break flow behavior of the experiment. However, due to the difference in the timing of the SG ADV opening, a reduction in discharge flow was observed at a point approximately 200s prior to the experiment.

In the ATLAS test, the LSC phenomenon was initiated by the DP between the HL (or core) and the CL (or DC), relying on the manometric force between the bottom of the loop seal and the water levels in the core or DC [16]. Due to the coolant supply to the core facilitated by the LSC, the excursion of the cladding temperature was delayed in the ATLAS test.

In the case of MARS-KS 3D, the first LSC phenomenon occurred in IL1A at approximately 1,600 seconds, resulting in a rapid increase in the core water level at around 1,600 seconds, as illustrated in Figure 4-10(a). Consistent with the experiment, the delay in the cladding temperature excursion was attributed to the coolant supply to the core facilitated by the LSC. In the MARS-KS 3D calculation, the second LSC phenomenon occurred in IL1B, IL2A, and IL2B around 2,080 seconds. This second LSC phenomenon led to a second temperature excursion of the cladding, as shown in Figure 4-10(b). However, since SITs were being injected at this point, the cladding temperature excursion was not as significant as observed during the first PCT.

Figure 4-4 illustrates the pressure in the primary system. The safety injection was intended to commence during the initial rapid depressurization once the set point in SIP was reached. However, in the 3D calculation, the SIP did not activate due to the previously mentioned LSI condition. The calculations from both codes not only demonstrated a gradual depressurization of the primary system due to LSI until the ADV opening as AM operation but also reasonably predicted the pressure behavior observed in the experiment.

As mentioned before, the SG ADV opened approximately 200 seconds prior to in the experiment, causing a rapid depressurization around 2,000 seconds. The SG ADV opens when the PCT exceeds 623.15 K, and the opening timing varies with the core collapsed water level behavior. Therefore, these results indicate that both code calculations exhibit a different core water level behavior from the experiment, which means that it is closely related to the phenomenon of LSC. Since loop seal behavior contributes to both the decrease and increase of the core water level, it directly influences the timing of core cooling.

Figures 4-5 and 4-6 depict the active core collapsed water level and PCT, respectively, in the 3D calculation. The reduction in the core collapse water level due to break flow and core boiling exposes the active core, increasing the PCT. When the PCT exceeded 623.15 K, an AM operation was initiated to open the ADV, enhancing cooling through the secondary system. This AM action led to the depressurization of the primary system to the setpoint of the SITs, initiating the injection by the SITs.

Figures 4-7, 4-8, and 4-9 illustrate the behavior of RCP side IL collapsed water level in both experimental and code simulations, respectively. The loop seal phenomenon was accurately captured in both the experiment and the system codes, albeit with slightly differing timing. In the experiment, the LSC phenomenon occurred specifically in IL2A around 1,850 seconds. This phenomenon contributed to a sudden increase in the core collapsed water level around 1,850 seconds, as depicted in Figure 4-10(a).

In the TRACE 3D calculation, partial LSC occurred followed by complete clearing, unlike the MARS-KS 3D calculation. Therefore, a sudden change in the collapsed water level was not observed, and it is judged that the core was relatively slowly heated, gradually decreasing. Although the onset of cladding temperature increases in the TRACE calculation occurred approximately 60 seconds earlier than in MARS-KS, it is considered that the opening timing of the SG ADV was delayed due to the reasons mentioned above. The differential pressure of steady state across the DC-HL in MARS-KS and TRACE codes was found to be 0.524 kPa and 0.477 kPa, respectively, with a minor difference. Additionally, the two codes have different critical flow models, leading to slightly differing break flow, and they include different physical models. Therefore, it is judged that the calculation results of the two codes may differ to some extent.

The FFTBM analysis results presented in Table 4-3 indicate that the two codes demonstrate similar predictive performance. The weighting factor was used to consider the different importance from the viewpoint of safety analysis and to calculate the overall accuracy of the calculation. In the present analysis, the weighting factors used are in line with the DSP FFTBM paper [17]. Based on comprehensive predictive capability indicators, the calculation results of each code were found to appropriately predict the behavior of the experiment. From these results, it can be confirmed that the 3D components of both codes exhibit similar predictive performance for system-scale phenomena and reasonably predict the behavior of the experiment.

Table 4-2 3D Chronology of the Transient Main Events

Event	Exp. (s)	MARS-KS (s)	TRACE (s)	Remarks
Break	0	0	0	Break valve open
LPP (Rx, RCP trip)	68	64	63	PT-PZR-01 < 10.72 MPa
MSIS	72	68	67	LPP Trip + 3.54 sec delay
MFIS	75	71	70	LPP Trip + 7.07 sec delay
Decay Heat	80	76	75	LPP Trip + 12.07 sec delay
AM Action	2192	2017	2044	PCT > 623.15K
ADV Open	2195	2017	2044	ADV 50% open
SIT Injection	2301	2089	2102	PT-DC-01 < 4.03MPa
SIT_FD (Low Flow)	2671	2406	2397	SIT Level < 2.0m
SIT_Termination	2998	2787	2854	SIT Level < 0.1m

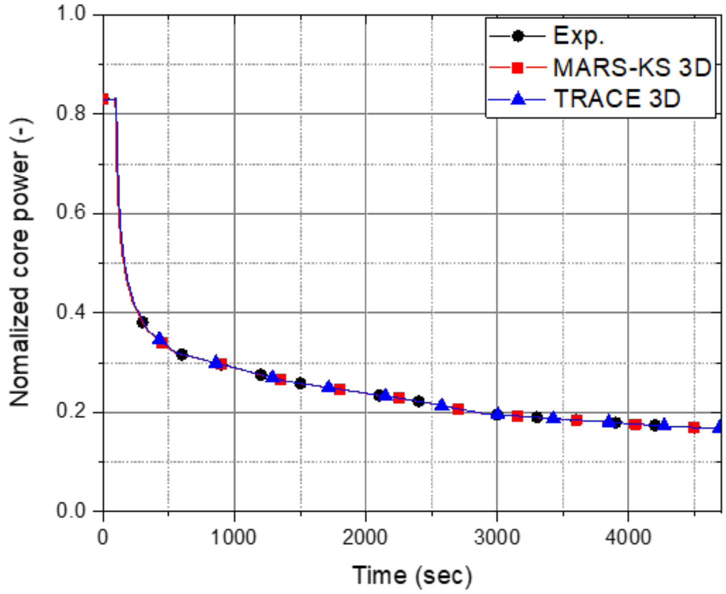

Figure 4-2 Power of the Core Heater (3D)

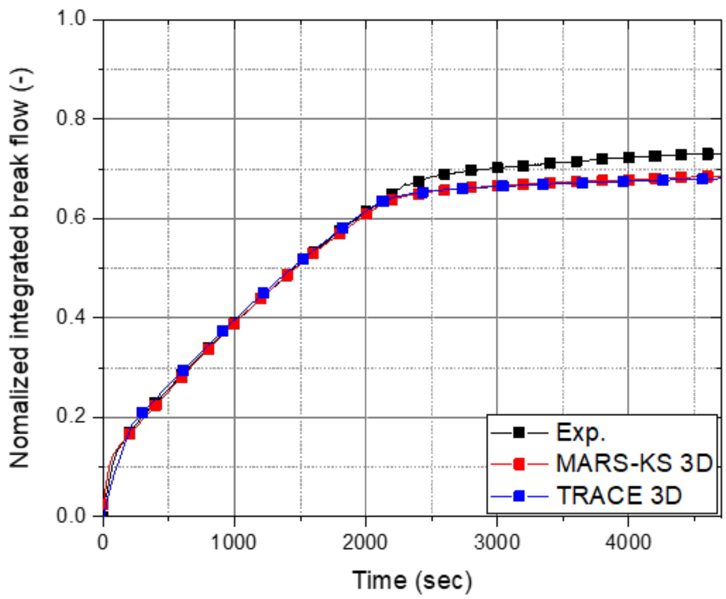

Figure 4-3 Integrated Break Flow (3D)

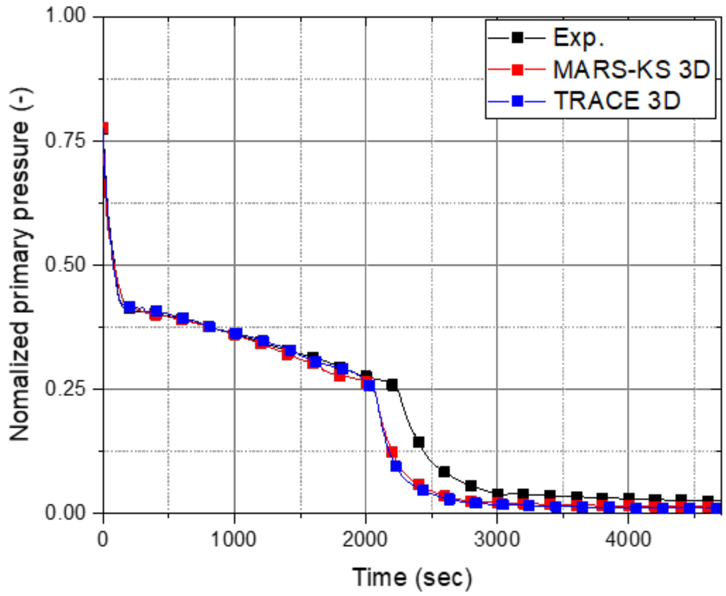

Figure 4-4 Pressure of the Primary System (3D)

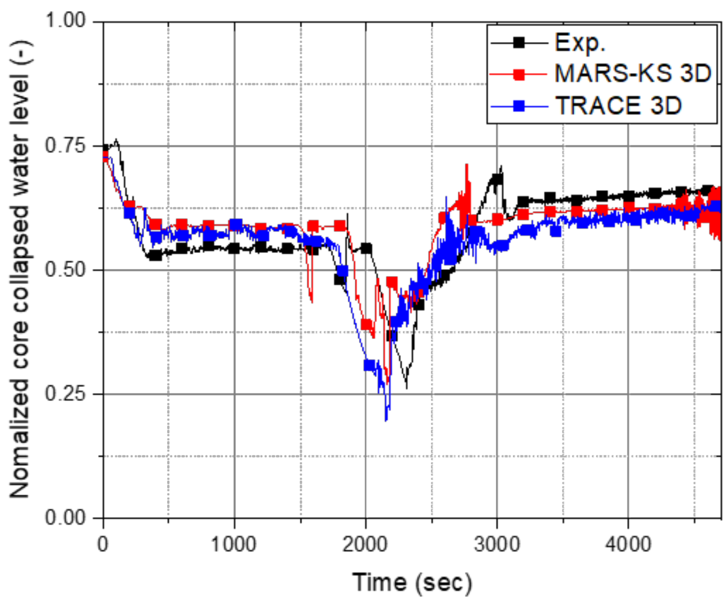

Figure 4-5 Active Core Collapsed Water Level (3D)

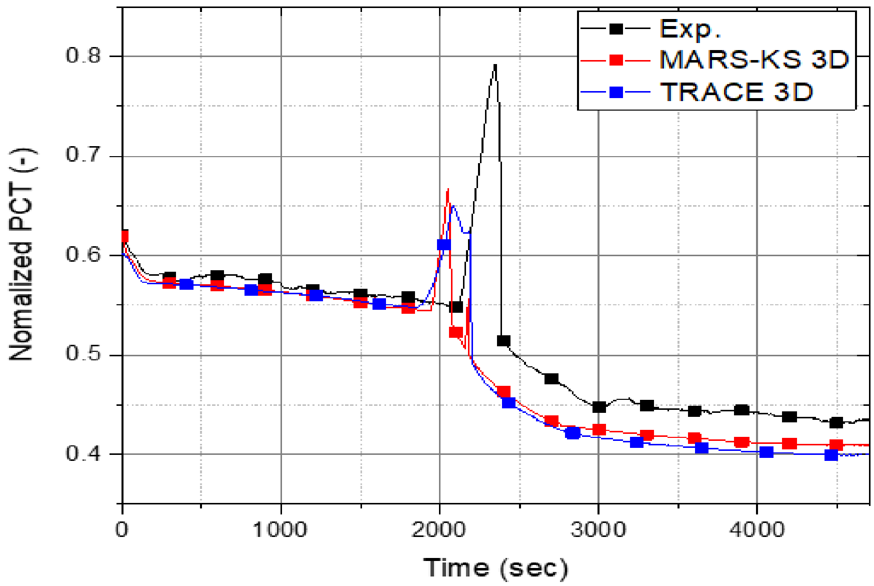

Figure 4-6 Peak Cladding Temperature (3D)

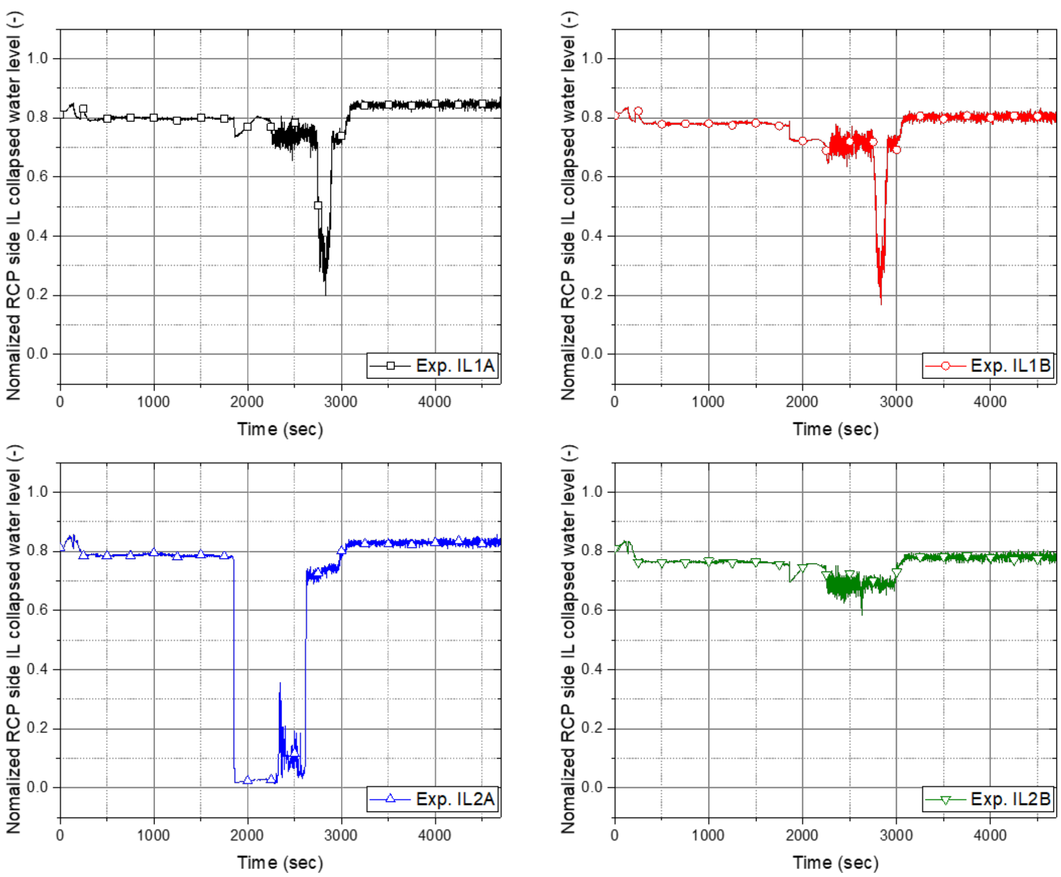

Figure 4-7 RCP Side IL Collapsed Water Level of Experiment

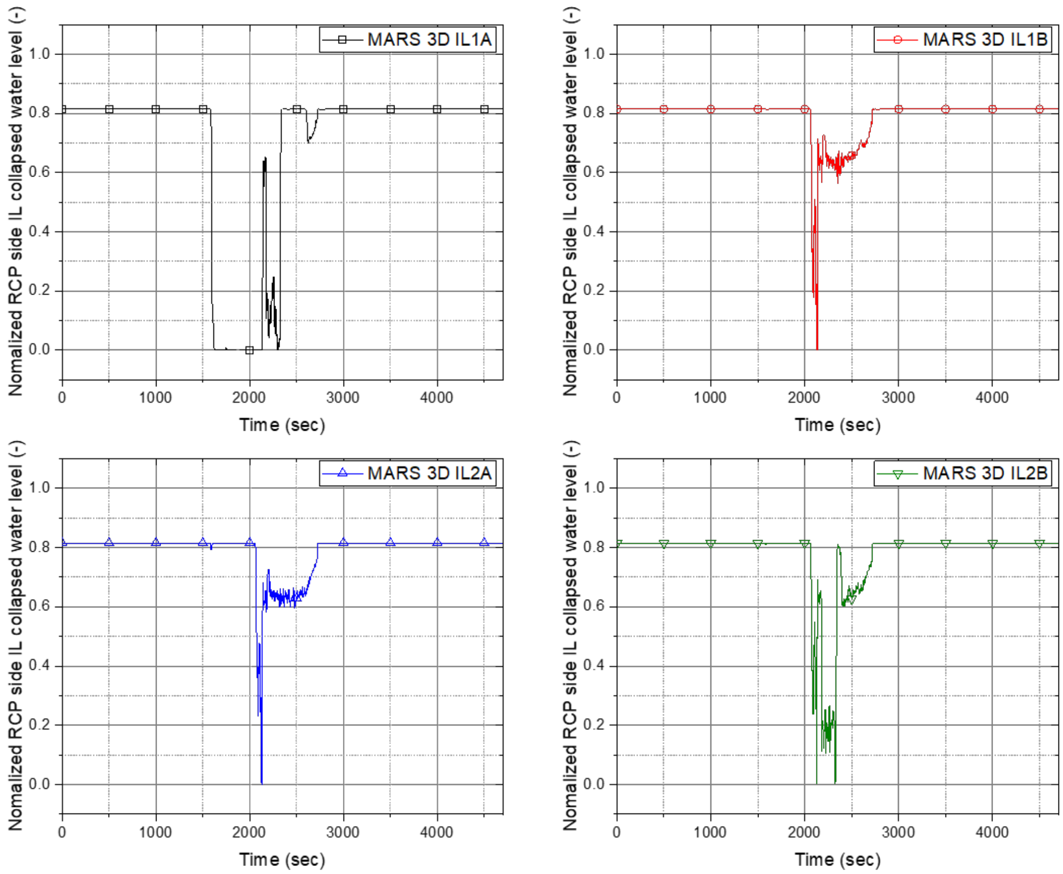

Figure 4-8 RCP Side IL Collapsed Water Level of MARS-KS (3D)

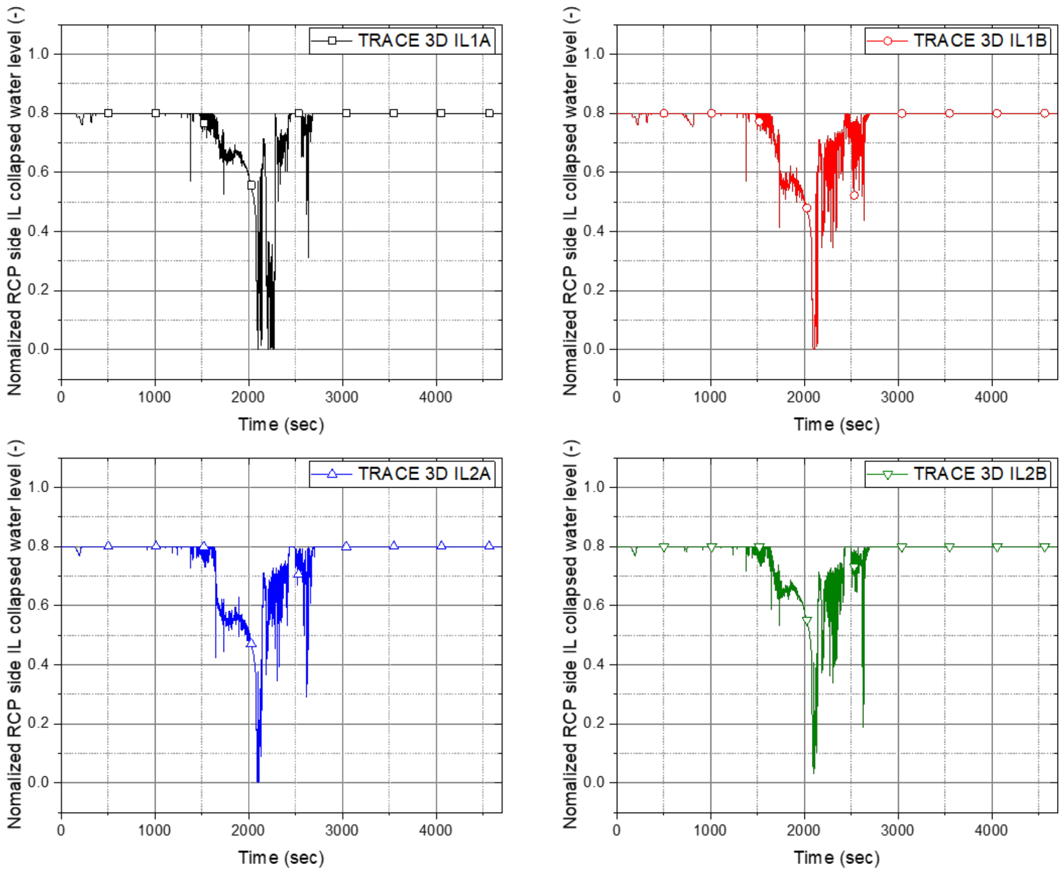

Figure 4-9 RCP Side IL Collapsed Water Level of TRACE (3D)

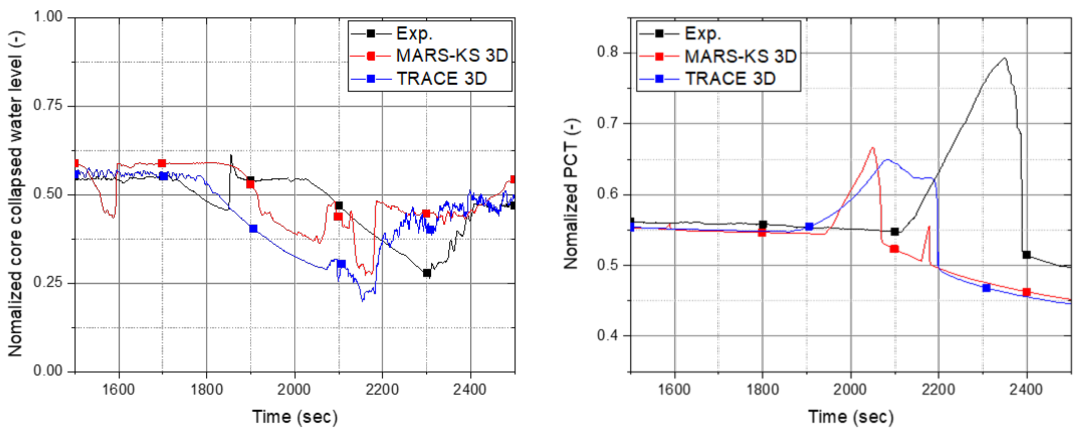

(a) Active core level

(b) PCT

Figure 4-10 Active Core Collapsed Water Level and PCT (1,500~2,500 Sec)

Table 4-3 Results of the FFTBM Analysis

Variable list	Average amplitude (AA)	
	MARS-KS	TRACE
Integrated break mass	0.061	0.061
Primary pressure	0.118	0.114
Core collapsed level	0.476	0.477
PCT	0.351	0.363
AA(Total)	0.248	0.250
Acceptability criterion		
AA(Total) ≤ 0.3	very good code prediction	
0.3 < AA(Total) < 0.5	good code prediction	
0.5 < AA(Total) < 0.7	poor code prediction	
0.7 ≤ AA(Total)	very poor code prediction	

5 CONCLUSIONS

An experiment for the CRDM nozzle rupture with LSI was conducted at the ATLAS. It was analyzed using both MARS-KS 3D and TRACE 3D in order to evaluate the predictability of both codes for the multiple failure accident with AM action. To ensure minimal modeling differences, the nodalization adopted an identical 3D component modeling approach for both codes. While the 3D ATLAS models of each code mirrored the 1D ATLAS modeling approach, they differed in the RPV model.

Additionally, preliminary 1D node sensitivity analysis evaluated the effects of stratification in the upper RPV head using varying numbers of nodes. The sensitivity analysis clearly revealed the limitations of the reference nodalization, emphasizing its significant impact on the analysis results. It underscored the importance of modeling that considers the physical phenomena occurring during transients. Hence, the 3D RPV modeling followed the same approach as the 1D nodalization for the RPV upper head, demonstrating that both codes accurately predicted the overall physical behaviors of the system during the accident.

The effect of the AM action was studied by modeling the ADV, and both codes' calculations yielded conclusions consistent with the experiment. Generally, the transient behavior in 3D for both codes exhibited similar system behavior, except for the formation of the loop seal and its impact on system behavior. In the 3D calculation for both codes, the integrated break flow and the primary system pressure behavior until ADV opening accurately replicated the experimental results. The timing of ADV opening directly correlated with core heat-up and the behavior of the active core collapsed water level, which varied based on loop seal behavior. Despite the 3D calculations of both codes portraying loop seal behavior slightly different from the experiment, they effectively captured the resulting physical phenomena from the loop seal.

6 REFERENCES

[1] K.J.Kim “Regulatory positions for in-service inspection,” Nuclear Safety & Security Information Conference *2015*, KINS, (2015).

[2] Nuclear Safety and Security Commission, “Special inspection status and future plans for identifying suspicions of maintenance of the reactor head of Hanbit Unit 5,” *129th Nuclear Safety and Security Commission*, 2020.

[3] K.H. Kang et al., “Test report on the small break loss of coolant accident simulation for the CEDM nozzle rupture with the ATLAS,” KAERI/TR-4856/2013, Korea Atomic Energy Research Institute 2013.

[4] J.B. Lee, B.U. Bae, Y. Park, J. Kim, S. Cho, N.H. Choi, K.H. Kang “Test result on a small break loss-of-coolant accident simulation for the control rod driving mechanism nozzle rupture with a failure of safety injection pump using the ATLAS facility,” Transactions of the Korean Nuclear Society Virtual Spring Meeting, May 13-14, 2021.

[5] Korea Institute of Nuclear Safety (KINS), MARS-KS Code Manual Volume I: Theory Manual, KINS/RR-1882 Vol.1, 2018.

[6] United States Nuclear Regulatory Commission (US NRC), TRACE V5.0 User’s Manual, 2008.

[7] W.P. Baek, C.-H. Song, B.J. Yun, T.S. Kwon. KAERI Integral Effect Test Program and ATLAS Design, Nuclear Technology 152, pp.183-195, 2005.

[8] K.Y. Choi, K.H. Kang, T.S. Kwon, Y.S. Kim, J. Kim, S.K. Moon, Y.S. Park, H.S. Park, B.U. Bae, C.H. Song, S.J. Yi, S. Cho, B.J. Yun, Scaling Analysis Report of the ATLAS Facility, Korea Atomic Energy Research Institute Technical Report, KAERI/TR-5465/2014 2014.

[9] Ishii, M., Kataoka I., Similarity Analysis and Scaling Criteria for LWRs Under Single Phase and Two-Phase Natural Circulation, NUREG/CR-3267, ANL-83-32, Argonne National Laboratory. 1983.

[10] J. Kim, K.H. Kang, B.U. Bae, Y. Park, A. Shin, M. Cho, “Evaluation for 4-Inch Cold Leg Top-Slot Break LOCA in ATLAS Facility with RELAP5 Mod3.3 Patch5”, NUREG/IA-0523, 2021.

[11] Choi, K.Y., et al., MARS Input Data for 8% Steady-State Calculation of the ATLAS, KAERI/TR-3046/2005, 2005.

[12] J.B. Lee, B.U. Bae, Y.S. Park, J. Kim, Y.S. Kim, S. Cho, W. Jeon, H.S. Park, S.J. Yi, S.K. Moon, K.Y. Choi, C.H. Song, N.H. Choi, Y.C. Shin, K.H. Min, K.H. Kang, Description report of ATLAS facility and instrumentation (second revision), Korea Atomic Energy Research Institute Technical Report, KAERI/TR-7218/2018. 2018.

[13] Henry, R.E., Fauske, H.K., McComas, S.T., Two-Phase Critical Flow at Low Qualities, Part I: Experimental, Nucl. Sci. Eng. 41, 79-91, 1970.

[14] J.A. Trapp, V.H. Ransom, “A choked-flow calculation criterion for nonhomogeneous, nonequilibrium, two-phase flows”, Idaho National Engineering Laboratory, April 27,1982.

[15] H. Jeong et al., “Analysis of MSGTR-PAFS Accident of the ATLAS using the MARS-KS Code”, J. Korean Soc. Saf., Vol. 36, No. 3, pp. 74-80, 2021.

[16] Y.S. Kim and K.H. Kang, ”Comparison of loop seal clearing behavior between SBLOCA and SBO-related tests in the ATLAS facility,” Annals of Nuclear Energy 132, 734-740, 2019.

[17] Y.S. Kim. et al., First ATLAS domestic standard problem (DSP-01) for the code assessment. Nucl. Eng. Technol. 43 (1), 25–44, 2011.

NRC FORM 335 (12-2010) NRCMD 3.7 U.S. NUCLEAR REGULATORY COMMISSION **BIBLIOGRAPHIC DATA SHEET** *(See instructions on the reverse)*	1. REPORT NUMBER (Assigned by NRC, Add Vol., Supp., Rev., and Addendum Numbers, if any.) **NUREG/IA-0552**
2. TITLE AND SUBTITLE **Analysis of CRDM Nozzle Break at the ATLAS Facility with 3D Components in MARS-KS and TRACE**	3. DATE REPORT PUBLISHED MONTH: **June** YEAR: **2025**
	4. FIN OR GRANT NUMBER
5. AUTHOR(S) Hyunjoon Jeong*, Taewan Kim*, Jae Soon Kim**, Dong Gu Kang**	6. TYPE OF REPORT Technical
	7. PERIOD COVERED (Inclusive Dates)

8. PERFORMING ORGANIZATION - NAME AND ADDRESS (If NRC, provide Division, Office or Region, U. S. Nuclear Regulatory Commission, and mailing address; if contractor, provide name and mailing address.)

*Incheon National University (INU),
119 Academy-ro, Yeonsu-gu, Incheon 22012, Republic of Korea
**Korea Institute of Nuclear Safety (KINS)
62 Gwahak-ro, Yuseong-gu, Daejeon 34142, Republic of Korea

9. SPONSORING ORGANIZATION - NAME AND ADDRESS (If NRC, type "Same as above", if contractor, provide NRC Division, Office or Region, U. S. Nuclear Regulatory Commission, and mailing address.)

Division of Systems Analysis
Office of Nuclear Regulatory Research
U.S. Nuclear Regulatory Commission
Washington, D.C. 20555-0001

10. SUPPLEMENTARY NOTES

A. Hsieh, NRC Project Manager

11. ABSTRACT (200 words or less)

The Korea Atomic Energy Research Institute (KAERI) operates the Advanced Thermal-Hydraulic Test Loop for Accident Simulation (ATLAS), an integral effect test facility designed based on the Advanced Power Reactor 1400 (APR1400) to simulate transient and design basis accidents. A loss of coolant accident (LOCA) test was conducted at the top of the reactor pressure vessel (RPV) at ATLAS to explore the impact of the loss of safety injections (LSI) and evaluate accident management (AM) actions during the anticipated accident. An analysis of the ATLAS Control Rod Drive Mechanism (CRDM) nozzle break experiment was performed using the MARS-KS and TRACE codes with their respective 3D components.
The primary objective of this study is to investigate thermal-hydraulic phenomena during a small break LOCA at the RPV upper head with LSI and assess the predictability of system analysis codes after AM actions during the test. The calculation results are compared and discussed not only against the experimental data but also with the calculation results of the VESSEL component, a 3D component of TRACE.

12. KEY WORDS/DESCRIPTORS (List words or phrases that will assist researchers in locating the report.)	13. AVAILABILITY STATEMENT unlimited
ATLAS, SBLOCA, LSI, Multiple Failure Accident, RPV Upper Head, MARS-KS, TRACE, MultiD Component, VESSEL Component	14. SECURITY CLASSIFICATION *(This Page)* unclassified *(This Report)* unclassified
	15. NUMBER OF PAGES
	16. PRICE

NUREG/IA-0552 Assessment of 3D Components in System Codes Against Separate Effect Tests June 2024